

# Millimeter-Wave True-Time Delay Array Beamforming with Robustness to Mobility

Benjamin W. Domae, Ibrahim Pehlivan, and Danijela Cabric

*Electrical and Computer Engineering Department,*

*University of California, Los Angeles*

Emails: bdomae@ucla.edu, ipehlivan@ucla.edu, danijela@ee.ucla.edu

**Abstract**—Ultra-reliable and low-latency connectivity is required for real-time and latency-sensitive applications, like wireless augmented and virtual reality streaming. Millimeter-wave (mmW) networks have enabled extremely high data rates through large available bandwidths but struggle to maintain continuous connectivity with mobile users. Achieving the required beamforming gain from large antenna arrays with minimal disruption is particularly challenging with fast-moving users and practical analog mmW array architectures. In this work, we propose frequency-dependent slanted beams from true-time delay (TTD) analog arrays to achieve robust beamforming in wideband, multi-user downlink scenarios. Novel beams with linear angle-frequency relationships for different users and sub-bands provide a trade-off between instantaneous capacity and angular coverage. Compared to alternative analog array beamforming designs, slanted beams provide higher reliability to angle offsets and greater adaptability to varied user movement statistics.

**Index Terms**—URLLC, beamforming, millimeter-wave, true-time delay array, joint phase time array

## I. INTRODUCTION

Future 6G cellular communications networks are developing ultra-reliable and low-latency communication (URLLC) capabilities to support applications that require high-reliability. Extended reality (XR), in particular, requires high data rates with extremely low latency and high reliability, as high latency bursts and connectivity disruptions can cause discomfort for users [1]. Millimeter-wave (mmW) and sub-terahertz (sub-THz) systems, operating at 30-300 GHz, can meet this demand for high data rates but must properly align narrow antenna array beams to maintain sufficient signal-to-noise ratio (SNR) for communications. For XR, consistent beam alignment (BA) is especially critical due to rapid user movement and rotation. Current mmW devices complete this BA over time using a periodic exhaustive search of all potential beams. However, these searches are undesirable for URLLC, as their latency scales linearly with array size due to narrower beams.

One way to reduce BA delay is to conduct BA less frequently. [2] and [3] increase the BA repetition period by predicting beams with Kalman filtering or machine learning respectively. This strategy reduces average BA delays over time but can leave gaps in coverage due to tracking inaccuracy or beam switching delays from array hardware. Wider beams

allow for less frequent beam updates by trading some beamforming gain for more angular coverage, enabling the same beam to be used for more time where a user may be moving. Increased angular coverage increases the beam's *robustness*, or resiliency to unknown angle offsets from movement or errors. Prior algorithms have utilized wider beams from smaller arrays [4], arrays with deactivated elements [5], or simplified models [6] for more efficient tracking. [5] and [6] each additionally optimized beamwidths for robustness to angle offsets.

True-time delay (TTD) arrays, also known as joint phase-time arrays (JPTAs), are simple analog phased arrays (PAs) arrays with added TTD elements that enable more flexible beamforming and faster BA. With a single RF chain, TTD arrays can control the frequency-dependence of their beam patterns [7]. In wideband scenarios, PA beams are also frequency-dependent from beam squint, but this angle-frequency relationship is not controllable. While fully-digital and hybrid arrays may also have frequency-dependent beamforming capability, their multiple RF chains can be expensive and power hungry. Several recent works have shown TTD arrays' promise for flexible wideband beamforming for orthogonal frequency-division multiple access (OFDMA) and fast BA [8]–[10]. TTD arrays have also been studied for robustness to mobility with frequency-stepped [11] and sector-dispersive [12] beams, but these methods are most efficient for single user cases.

In this work, we propose a robust downlink beamforming design using functionally-wider beams from analog-TTD arrays. Our *slanted beams* solution creates beams with approximately linear angle-of-departure (AoD)-to frequency relationships, like [8] and [12], but over specified angle sectors associated with contiguous sub-bands for multi-user OFDMA. Slanted beams provide a way to trade-off capacity per user for mobility robustness; steeper slopes in the AoD-frequency domain cover more AoDs but have fewer strong subcarriers in each sub-band. We design the angular range to meet specified robustness requirements, providing a reliable but heavily frequency-faded channel over each user's sub-band.

The remainder of this work is organized as follows: Section II discusses our system model, problem statement, and metrics. Section III details the selected baseline beamforming and our proposed slanted beams design, while Section IV presents our simulation results comparing slanted beams to the baseline beams. Finally, we conclude in Section V.

*Notation:* Scalars, vectors, and matrices are represented by

This material is based upon work supported by the National Science Foundation under Grant No. 2224322.

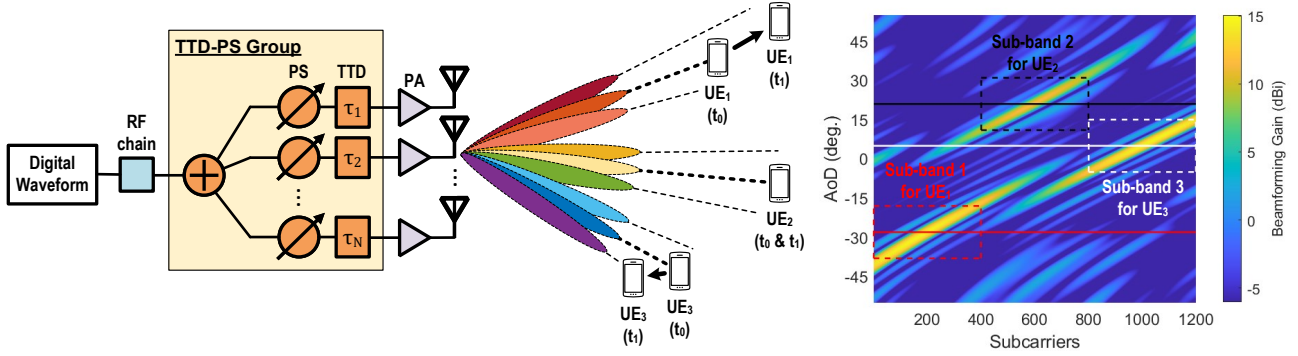


Fig. 1. System architecture with three users (and three sub-bands) with a corresponding example slanted beams pattern.

non-bold, bold lowercase, and bold uppercase letters respectively. The  $i$ th entry of  $\mathbf{a}$  is denoted as  $\mathbf{a}_i$ . For  $\mathbf{A}$ , the  $i$ th row is  $[\mathbf{A}]_{i,:}$  and the  $j$ th element of the  $i$ th row is  $[\mathbf{A}]_{i,j}$ . The transpose and Hermitian transpose of  $\mathbf{A}$  are  $\mathbf{A}^T$  and  $\mathbf{A}^H$  respectively.

## II. SYSTEM MODEL AND PROBLEM STATEMENT

We consider a URLLC downlink (DL) mmW OFDMA system, where a base station (BS) beamforms towards each potentially-moving user equipment (UE) and sends each UE's continuous data stream on separate sub-bands. While higher data rates are better, our primary objective is to maintain a highly-reliable minimum data rate at all times for all UEs. An overview of our system is shown in Fig. 1 with three users.

### A. True-Time Delay Array Beamforming and SINR

The analog TTD array architecture is key to our unique slanted beams. Fig. 1 shows the BS transmitter (Tx) TTD array architecture. Each antenna element has one TTD and one phase shifter (PS), enabling controlled beam squint through the combination of frequency-independent time delays and frequency-dependent phase shifts. The TTD beamforming antenna weight vector (AWV) for a vector of delays  $\tau \in \mathbb{R}^{N_t}$  and vector of phases  $\phi \in \mathbb{R}^{N_t}$  can be expressed for antenna element  $n$  and frequency  $f$  as (1), where  $N_t$  is the number of BS antennas. The gain pattern for this AWV at AoD  $\theta$  and frequency  $f$  is then shown in (2) with  $d$ -wavelength antenna spacing, center frequency  $f_c$ , speed of light  $c$ , and array response  $\mathbf{a} \in \mathbb{C}^{N_t}$ ,  $\mathbf{a}_n(\theta, f) = \exp(j2\pi(n-1)\sin(\theta)f_c d/c)$ .

$$\mathbf{v}_n(f) = \exp(j(\phi_n - 2\pi\tau_n f)) \quad (1)$$

$$a(\theta, f) = |\mathbf{a}^H(\theta, f)\mathbf{v}(f)|^2 \quad (2)$$

$$\mathbf{y}(u, t_i) = [\mathbf{H}_u \tilde{\mathbf{P}}_i \mathbf{x}]_{\kappa_u} + n_u[i] \quad (3)$$

$$[\mathbf{H}_u(t_i)]_{k,k} = h_u \mathbf{a}^H(\theta_u(t_i), f_k) \mathbf{v}(f_k) \quad (4)$$

For UE  $u$  at AoD  $\theta_u$  and time step  $t_i$ , the  $K/U$  received symbols from the TTD BS are described in (3) without frequency offsets, where  $n_u[i]$  is additive Gaussian white noise (AWGN) with variance  $\sigma_N^2$ . We assume a sequential association of users to sub-bands, so  $\kappa_u = \left\{ \frac{(u-1)K}{U} + 1, \dots, \frac{uK}{U} \right\}$  are the subcarrier indices for user  $u$ . UE  $u$ 's channel is assumed to be entirely line-of-sight (LOS), so  $\mathbf{h}_u(t_i, f) = h_u \mathbf{a}(\theta_u(t_i), f)$ , where  $h_u$  is the channel propagation loss. The raw symbols  $x \in \mathbb{C}^K$  are normalized to have unit average

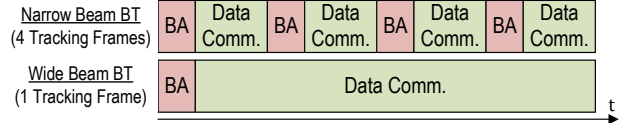


Fig. 2. One data communication beam is used per BA frame. With 5G-NR parameters, wide beam tracking frames could be up to 16 times as long as those of narrow beams, requiring fewer BA interruptions.

power, with the Tx power allocation is  $\mathbf{P} \in \mathbb{R}^{R \times K}$ , where  $\mathbf{P}_i = \text{diag}([\mathbf{P}_{i,1}, \dots, \mathbf{P}_{i,K}])$ .

The beamforming frequency fading is given in the  $K \times K$  diagonal matrix  $\mathbf{H}_u(t_i, f)$  (4). OFDMA subcarrier orthogonality, spatial and frequency filtering from the beamforming, and our LOS channel assumption effectively eliminate inter-carrier and inter-user interference without frequency offsets. The nominal SNR, without Tx array gain, is  $\psi = P_{\text{tot}}/\sigma_N^2$ , where  $P_{\text{tot}}$  is the total power of the transmitted OFDMA symbol. The total SNR with Tx beamforming is given as  $\zeta_{k_u}(t_i) = |[\mathbf{H}_u \tilde{\mathbf{P}}_i]_{k_u, k_u}|^2 \frac{K}{\sigma_N^2}$ , for user  $u$ 's subcarrier  $k_u$ .

### B. BA Frames and Movement Model

In this work, we design a single beamformer to downlink to multiple UEs during a single BA frame, or a period of  $T$  seconds between subsequent BAs. In 5G New Radio (5G-NR), this is equivalent to designing a single data communications beam for the period  $T$  between Synchronization Signal Blocks (SSBs), between 10-160 ms and typically 20 ms [13]. As shown in Fig. 2, increasing  $T$  reduces interruptions to data communications for BA overhead. However, higher  $T$  could reduce tracking quality, as each UE has more time to move outside of the beam. For our simulations, we break a BA frame  $T$  into  $R$  time steps of length  $\Delta t = T/R$ .

Our random movement model for user  $u$  is shown in (5). Due to the relatively short time scale of each BA frame, we simplified each UE's randomized movement over a frame to a one-dimensional angular kinematics model. UE  $u$ 's kinematics, AoD  $\theta_u(t)$ , angular velocity  $\omega_u(t)$ , and constant angular acceleration  $\alpha_u$ , are parameterized by random variables for their initial conditions. We assume a separate earlier algorithm provides unbiased estimates for  $u$ 's initial conditions, denoted as  $\hat{\theta}_u(t_0)$ ,  $\hat{\omega}_u(t_0)$ ,  $\hat{\alpha}_u$ . We further assume the estimation error is Gaussian-distributed with variances  $\sigma_\theta$ ,  $\sigma_\omega$ , and  $\sigma_\alpha$  respectively. The unknown errors create a Gaussian distribution of  $\theta_u(t_i)$ , the possible AoDs for each user at each time step,

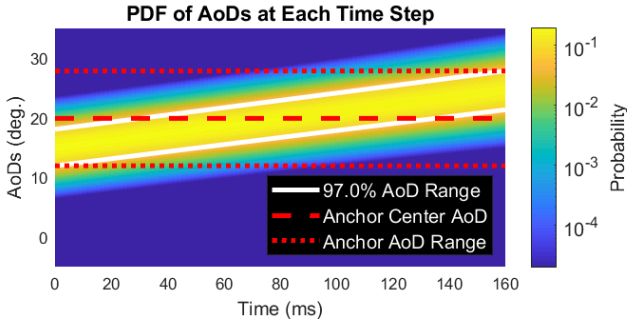


Fig. 3. Example AoD range and anchor selection for one user with  $P=97\%$ ,  $\hat{\theta}_u(t_0)=15^\circ$ ,  $\hat{\omega}_u(t_0)=60$  deg/s. See Table II for the remaining parameters.

with mean (6) and variance (7). Fig. 3 illustrates an example of the density of this distribution.

$$\theta_u(t_i) = \theta_u(t_0) + (i\Delta t)\omega_u(t_0) + (i\Delta t)^2 \frac{\alpha_u}{2} \quad (5)$$

$$\hat{\theta}_u(t_i) = \hat{\theta}_u(t_0) + (i\Delta t)\hat{\omega}_u(t_0) + (i\Delta t)^2 \frac{\hat{\alpha}_u}{2} \quad (6)$$

$$\sigma_i = \sigma_\theta + (i\Delta t)^2 \sigma_\omega + (i\Delta t)^4 \frac{\sigma_\alpha}{4} \quad (7)$$

### C. System Capacity Metric

The primary system metric used in this work is the minimum channel capacity for all users over all time steps. In this work, we approximate a given user's capacity at discrete time steps  $t_i$  over a tracking frame using the receiver (Rx) SNR at the centers of all subcarriers  $f_k$ . The user capacity at time step  $i$  depends on the AoD to the user and the BS beamformer  $\mathbf{v}$ , as described in (8). The subcarrier spacing is  $w_{sc} = W/K$ , for total system bandwidth  $W$  and  $K$  subcarriers.

$$C_u(t_i, \mathbf{v}) = \sum_{k=1}^K C_{u,k}(t_i, \mathbf{v}) \quad (8)$$

$$C_{u,k}(t_i, \mathbf{v}) = w_{sc} \log(1 + \zeta_{k_u}) \quad (9)$$

$$= w_{sc} \log\left(1 + \mathbf{P}_{i,k} |h_u \mathbf{a}^H(\theta_u(t_i), f_k) \mathbf{v}(f_k)|^2 \frac{1}{\sigma_N^2}\right) \quad (10)$$

$$= w_{sc} \log\left(1 + \mathbf{P}_{i,k} a(\theta_u(t_i), f_k) \frac{1}{\sigma_N^2}\right)$$

### D. Problem Statement

Our objective is to design BS TTD beams that maximize the minimum capacity given random UE movement. This requires the system to maximize the continuously-available capacity for all UEs and time steps. This can be expressed as a non-convex optimization problem in (11), with physical constraints on the beamformer  $\mathbf{v}$ , power allocation  $\mathbf{P}$ , and maximum TTD  $\tau_{\max}$ .

$$\max_{\phi, \tau, \mathbf{P}} \min_{u,i} C_u(t_i, \mathbf{v}), \quad i \in \{1, \dots, R\}, u \in \{1, \dots, U\} \quad (11)$$

$$\text{s.t. } \phi_n \in [-\pi, \pi], \quad \tau_n \in [0, \tau_{\max}] \quad \forall n \in \{1, \dots, N_t\}$$

$$\mathbf{P}_{i,k} \geq 0 \quad \forall i, k$$

$$\sum_k \mathbf{P}_{i,k} = P_{\text{tot}} \quad \forall i$$

## III. TTD SLANTED BEAM DESIGN

### A. Proposed Slanted Beam Design

The optimization in (11) is nontrivial and would require a computationally-complex iterative algorithm to solve directly. Instead, our proposed slanted beams approximate the solution to (11) with a simple heuristic. For large arrays ( $N_t \gg 1$ ),

UEs at AoDs without main-lobe beamforming gain at any subcarriers within their sub-band will have insufficient SNR. In other words, to achieve a higher minimum capacity in (11), the designed beamformer must point towards each UE for some subcarriers in their respective sub-bands. This simplification of the problem allows us to instead design a heuristic beam that points a fraction of the bandwidth towards every AoD from a set of angles that will contain all UEs with selected probability  $p$ . The simplest form of beam pointing directions is a line of directions over the AoD-frequency domain of each user's AoD range and sub-band. The slope of this line provides a direct trade-off between supported AoD range and the number of subcarriers with significant beamforming gain, since the thickness or beamwidth of the line and the cross-section through the line at each subcarrier determine the capacity provided to a user at every angle. To maximize the minimum capacity, we thus aim to minimize the supported AoD range and the slope for every user.

To design slanted beams, we first select an AoD-frequency *anchor* for each user, or the combination of an AoD center  $\bar{\theta}_u$ , AoD range  $r$ , and sub-band that define each user's slanted beam. Since we assume user movement  $\theta_u(t_i)$  is Gaussian distributed with mean and variance given in (6) and (7) respectively, we use the Q-function to find  $\Theta_{u,i}$ , the smallest set of  $\theta_u(t_i)$  with selected probability  $p$ . Each user's individual center AoD  $\bar{\theta}_u$  and range  $r_u$  are then the median and range of  $\Theta_u$ , the union of all  $\Theta_{u,i}$ . The final range  $r$  used by all users is the maximum of all  $r_u$ . Each UE beam must use the same AoD-frequency slope, since TTD arrays are, to the authors' best knowledge, incapable of creating split beams with a different slope per sub-band. Fig. 3 demonstrates this selection for one user, where the red dashed lines of the anchor AoD range edges cover the maximum and minimum of the required range  $r$  for  $p=97\%$ , shown with white lines. Algorithm 1 describes the anchor design based on  $\mathbf{g} \in \mathbb{R}^K$ , the target directions for each subcarrier (12).

$$\mathbf{g}_{k_u} = \bar{\theta}_u + \frac{r}{2} - r u + \frac{r U}{K} k_u, \quad k_u \in \kappa_u \quad (12)$$

Finally, to generate our target slanted beam, we use the JPTA algorithm [9] to synthesize an AWV for a TTD array. This algorithm iteratively optimizes the TTDs and phase shifts to point the beam's main lobe towards a provided target  $\mathbf{g}_k$ ,  $k \in \{1, K\}$ . Effectively, the JPTA algorithm solves the following optimization problem:

$$\max_{\phi, \tau} \sum_{k=1}^K \left| \mathbf{v}_k^H \frac{\mathbf{a}(\mathbf{g}_k, f_k)}{\|\mathbf{a}(\mathbf{g}_k, f_k)\|} \right| \quad (13)$$

$$\text{s.t. } \phi_n \in [-\pi, \pi], \quad \tau_n \in [0, \tau_{\max}] \quad \forall n \in \{1, \dots, N_t\}$$

As (13) is non-convex, JPTA utilizes an alternating minimization with a Taylor approximation to approach a local optimum,  $\phi_n^*, \tau_n^*, \forall n$ . Based on our anchor design, we select a line of targeted pointing angles for each subcarrier in each user's sub-band and AoD sector. JPTA then optimizes the PS and TTD weights for this vector of target directions.

In this work, we assume a uniform power distribution for subcarrier water-filling. Since the true movement of the users is

---

**Algorithm 1** Slanted Beams Design Algorithm
 

---

**Inputs:**  $\hat{\theta}_u(t_0), \hat{\omega}_u(t_0), \hat{\alpha}_u, \sigma_\theta, \sigma_\omega, \sigma_\alpha, \forall u \in \{1, \dots, U\}$   
**Output:** Slanted TTD Beam  $\mathbf{v}(f)$

**select randomly** UE sub-band assignment  
 $\ell = Q(1 - \frac{1-P}{2})$   
**for** user  $u \in [1, \dots, U]$   
   **for** time step  $i \in [1, \dots, N_s]$   
     Compute movement  $\hat{\theta}_u(t_i)$  (6) and  $\sigma_i$  (7)  
      $\Theta_{u,i} = [\hat{\theta}_u(t_i) - \sqrt{\sigma_i}\ell, \hat{\theta}_u(t_i) + \sqrt{\sigma_i}\ell]$   
      $\Theta_u = \bigcup_{i=1}^{N_s} \Theta_{u,i}$   
      $r_u = \max(\Theta_u) - \min(\Theta_u) = \text{user } u \text{ AoD range}$   
      $\bar{\theta}_u = r_u/2 + \min(\Theta_u) = \text{user } u \text{ AoD anchor center}$   
      $r = \max_u(r_u) = \text{AoD anchor range}$   
     Select target AoDs  $\mathbf{g}$  for all sub-bands using  $\bar{\theta}_u, r$  in (12)  
     Solve for phases  $\phi$  and delays  $\tau$  using JPTA [9] with  $\mathbf{g}$   
     Create a beam  $\mathbf{v}$  from  $\phi$  and  $\tau$  using (1)  
**return**  $\mathbf{v}(f)$

---

not known prior to beamforming or transmission, the effective frequency fading from the slanted beams is also unknown. A uniform power allocation is intuitively reasonable, as it guarantees that all AoDs within the required range will have an equal capacity. However, a formal proof for the optimal power allocation strategy is left for future work.

### B. Baseline Analog Beamforming

Several analog beamforming approaches can be used to attempt to provide reliable coverage to multiple users through distinct OFDMA sub-bands. Table I summarizes all the included reference beams. In this work, we provide two primary baseline beam designs: stepped TTD beams and rainbow beams. Stepped TTD beams [9], [10] split non-dispersive beams towards each user's initial AoD estimate  $\hat{\theta}_u(t_0)$  over their entire sub-band. Since stepped beams are equivalent to slanted beams with  $r = 0$ , we use JPTA to design the AWVs. Dispersive rainbow beams [8] spread beam pointing directions across the entire AoD range over the entire bandwidth, presenting the asymptotic equivalent of slanted beams as  $U \rightarrow \infty$  and user sub-band associations are sorted by AoD.

We also include three baseline designs that are not practical for this system but demonstrate the benefits of slanted beams. The two *genie* baselines require unrealistic *genie* knowledge of  $\theta_u(t_i)$ , the true AoDs of all UEs at all time steps. The stepped genie points a TTD stepped beam to all  $\theta_u(t_i)$  instead of the initial estimates  $\hat{\theta}_u(t_0)$ . This beam provides among the best performance available from a TTD array, though we will later show stepped beams may be sub-optimal for large numbers of users. The optimal genie uses a digital array beamformer to point perfect sub-band beams to all  $\theta_u(t_i)$ , providing maximum performance for any array of this size. Though a digital array could beamform the entire bandwidth to every user independently, we assume that the users must only use their own sub-band for a fair comparison with the

TABLE I  
COMPARISON OF BEAMFORMING METHODS

Beam	Array	Width	AWV or Phases and Delays
<i>Slanted</i>	TTD	Wide	See Algorithm 1
Rainbow	TTD	Wide	$\tau_n = -n/(2B)$ , $\phi_n = 2\pi n f_c / W$
Stepped	TTD	Narrow	JPTA with $\mathbf{g}_{k_u} = \hat{\theta}_u(t_0)$
Stepped Genie	TTD	Narrow	JPTA with $\mathbf{g}_{k_u}(t_i) = \theta_u(t_i)$
Optimal Genie	Digital	Narrow	$\mathbf{v}_n(t_i, f_k) = N_t^{-1/2} \times$ $\exp j2\pi d \frac{f_k}{c} \sin \hat{\theta}_u(t_i)$
QPD ( $\Phi_m = \pi$ )	PA	Wide	$\phi_n = \frac{2\pi d f_c}{c} \sin(\hat{\theta}_1(t_0)) + \phi_{q,n}$ $\phi_{q,n} = 4\Phi_m \left( \frac{2n - N_t - 1}{2(N_t + 1)} \right)^2$

TABLE II  
SIMULATION PARAMETERS

Parameter	Value
Center frequency ( $f_c$ )	60 GHz
Bandwidth ( $W$ )	2 GHz
Number of subcarriers ( $K$ ) / Bandwidth ( $w_{sc}$ )	1200 / 1.67 MHz
Number of Tx antennas ( $N_t$ )	32
Antenna spacing ( $d$ )	$0.5\lambda$
SNR w/o beamforming	-10 dB
Initial AoD estimate range (for $\hat{\theta}_u(t_0)$ )	$[-45^\circ, 45^\circ]$
Minimum initial UE AoD spacing	$10^\circ$
Number of UEs ( $U$ )	3
BA frame time ( $T$ )	160 ms
Step time ( $\Delta t$ ; for $R = 100$ steps)	1.6 ms
Coverage probability parameter ( $p$ )	97%
Initial AoD error variance ( $\sigma_\theta$ )	$2 \text{ deg}^2$
Mean initial angular velocity range ( $\hat{\omega}_u(t_0)$ )	$[0, 80] \text{ deg/s}$
Initial angular velocity variance ( $\sigma_\omega$ )	$10 \text{ deg}^2/\text{s}^2$
Mean constant angular acceleration ( $\hat{\alpha}$ )	$0 \text{ deg}^2/\text{s}^2$
Constant angular acceleration variance ( $\sigma_\alpha$ )	$5 \text{ deg}^2/\text{s}^4$

analog beams. Finally, quadratic phase distribution (QPD) [14] beams provide a heuristic method to efficiently create single-lobe wide beams PAs. As a single-user beam design, QPD beams represent a lower limit for robust beamformer design.

## IV. SIMULATION RESULTS

Our simulation system parameters, unless otherwise specified for parameter sweeps, are shown in Table II for our 100 Monte Carlo (MC) trials comparing beamforming performance. These parameters were selected to provide realistic mobility and error. The initial AoD error variance is based on sub-beamwidth BA accuracy for the 32-element array's  $3.2^\circ$  beams. For a UE 3m from the boresight of the BS array, the 3.2 m/s maximum velocities found in experimental data [1] corresponds to 47 deg/s angular velocity. We select the maximum 5G-NR tracking frame length,  $T = 160$  ms, saving 7/8 BAs compared to a typical 20 ms 5G-NR SSB period. We target high-resolution XR requirements [15] including 100 Mbps DL per-user data rate and 99.99% end-to-end reliability.

Before discussing the capacity performance results, we provide example antenna patterns from the gamut of beam designs. Fig. 4 shows the gain from the 6 different beams as heatmaps over the AoD-frequency domain. The beams were designed for a scenario with a random AoD for each of 8

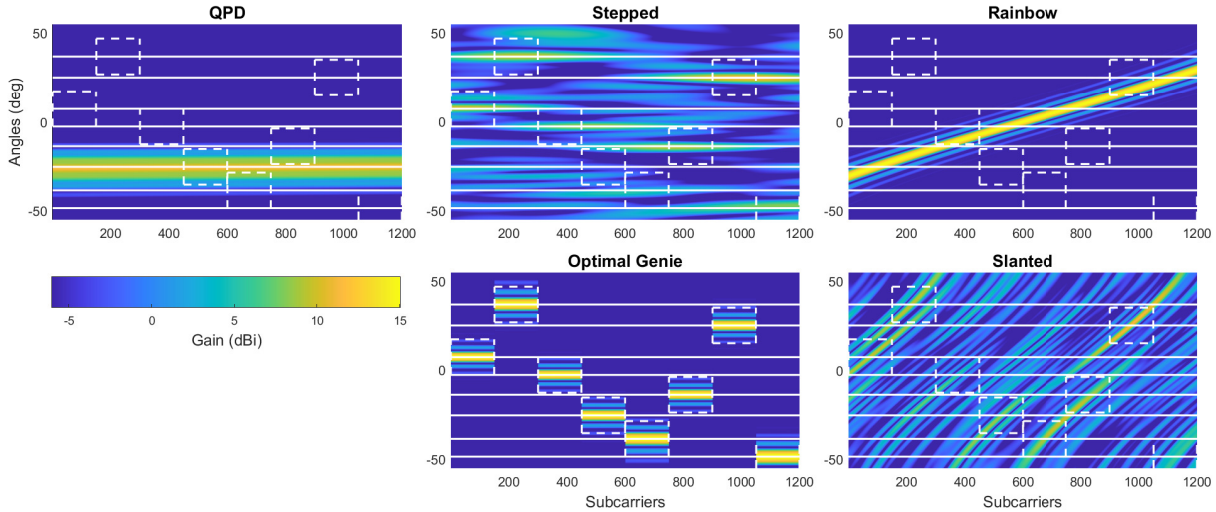


Fig. 4. Example comparison of all beam designs with  $U = 8$ , with the user anchors marked in white.

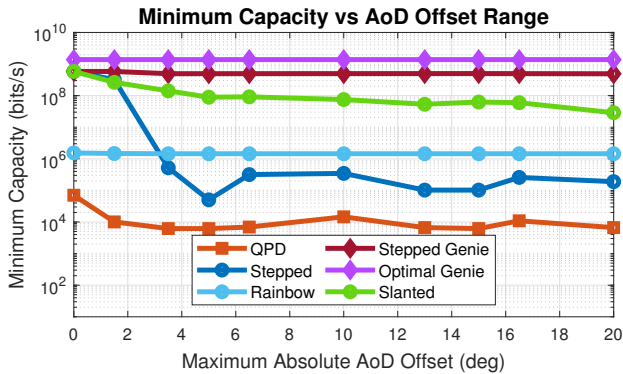


Fig. 5. Robustness of capacity to larger maximum AoD offsets.

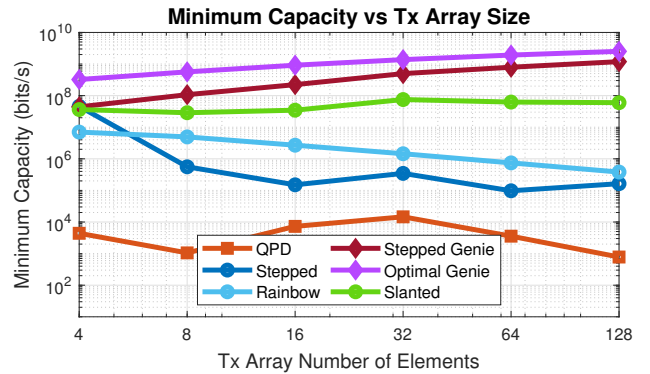


Fig. 6. Impact of Tx array size on robustness to AoD offsets.

users. For this plot, the genie beams only show the pattern designed for the center AoD, as these beams adjust for every true AoD. Compared to the 3 user example in Fig. 1, we see many additional side lobes as diagonal striations in the heatmap. This is expected, as the 32-element array averages only 4 antennas per user to service the 8 users simultaneously.

#### A. Minimum Capacity with Random AoD Offsets

Our first set of simulation results demonstrate slanted beams' robustness to random UE AoD errors from BA error or unmeasured movement and uncover the circumstances where slanted beams are most beneficial. Except in Fig. 5, the beams in this section were designed with a range  $r = 20^\circ$ . We computed the capacity per user over a grid of 100 uniformly-spaced angle offsets centered on the random UE AoDs for each MC trial. We use the *minimum capacity* metric,  $M = \min_{u,i} C_u(t_i, \mathbf{v})$ , to measure the minimum total capacity summed over sub-band subcarriers among all users and tested angle offsets. Fig. 5 shows  $M$  for each beam design as the range of AoD offsets,  $\theta_u - \hat{\theta}_u$ , increases from  $\pm 0^\circ$  to  $\pm 20^\circ$ . Slanted beams operate as designed; they show little degradation in  $M$  with larger offsets and provide the best result besides genie methods. As we will see in all results, the stepped genie beams perform well but are always worse than the digital genie beams. Rainbow beams provide consistent

$M$  at all offset ranges as they are independent of user AoDs. Unsurprisingly,  $M$  for stepped and QPD beams is the lowest for large angle offsets, as stepped beams narrowly focus on  $\hat{\theta}_u$  while QPD beams are only designed for one of three users.

We compare the beam designs' minimum capacity for random AoD offsets and varied BS array sizes in Fig. 6. Slanted beams provide consistent  $M$  over array sizes, since larger  $N_t$  provides higher peak gain but narrower supported bandwidth. The frequency cross-section of the angled linear beam pattern governs the effective bandwidth for a given AoD. Rainbow beams degrade  $M$  by orders-of-magnitude for larger  $N_t$ , as the narrower beams reduce their effective angle-frequency coverage. Genie beams have the true AoDs, do not follow this tradeoff, and improve with larger  $N_t$ . All other beams show even lower  $M$ , making slanted beams the only practical design to handle AoD uncertainty with large  $N_t$ .

Fig. 7 demonstrates how well the beam designs scale with more simultaneous users. Slanted beams are consistent again, even outperforming the genie TTD stepped beams when  $U = 8$ . As illustrated in Fig. 4, analog arrays struggle to produce beams with multiple distinct main lobes for many users. With our simulation parameters,  $U \geq 8$  reduces stepped beams' gain to where they are no longer optimal for OFDMA. We also found that the genie information is less relevant for TTD stepped beams with larger  $U$ . Stepped beams smear more

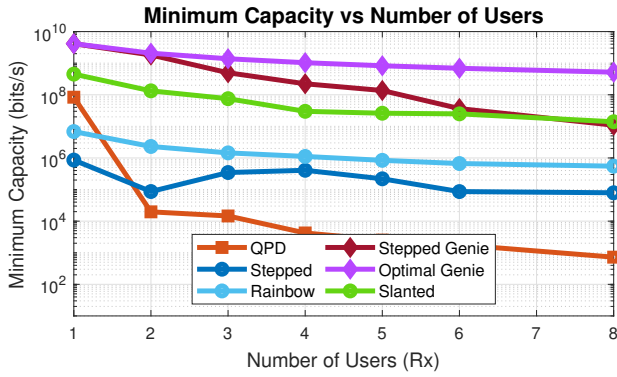


Fig. 7. Robust beamforming performance vs number of users.

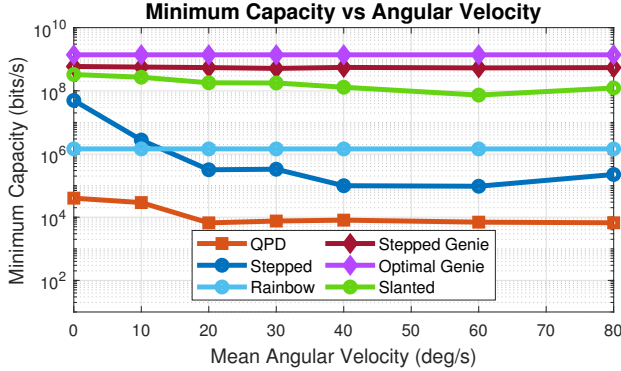


Fig. 8. Minimum capacity with increased UE velocity.

across AoDs reducing the stepped genie performance. While the optimal digital beamformer also degrades with larger  $U$ , as the bandwidth per user decreases, the stepped genie beams degrade much faster.

### B. Minimum Capacity with Random Movement

Finally, we show the performance of slanted beams with UE movement. In Fig. 8, we sweep mean initial angular velocities  $\hat{\omega}_u(t_0)$  to test faster movement. The minimum capacity results are similar to Fig. 5, since the random motion introduces a different AoD offset at each time step, larger velocities increase the range  $r$ , and thus beam robustness to larger  $\hat{\omega}_u(t_0)$  is robustness to larger AoD offsets. As in Fig. 5, slanted beams provided one to two orders-of-magnitude better  $M$  than the next best beams, rainbow beams. Slanted beams also provide higher capacity in more scenarios than the minimum. The capacity cumulative density functions (CDFs) in Fig. 9 summarize all MC trials, with its x-intercepts presenting select results from 8. For the three mean velocities shown, the proposed slanted beams *always* met the target 100 Mbps capacity, while the stepped and rainbow beams did not in 5%-75% of cases. At high velocities, slanted beams also provided higher capacity than stepped beams for most trials; 65% and 80% of cases for 40 deg/s and 80 deg/s respectively.

## V. CONCLUSION AND FUTURE WORK

In this paper, we propose TTD array based slanted beams, a novel method to create wideband, downlink beamforming that is robust to randomized user movement. The proposed beam design algorithm provides a simple tradeoff between

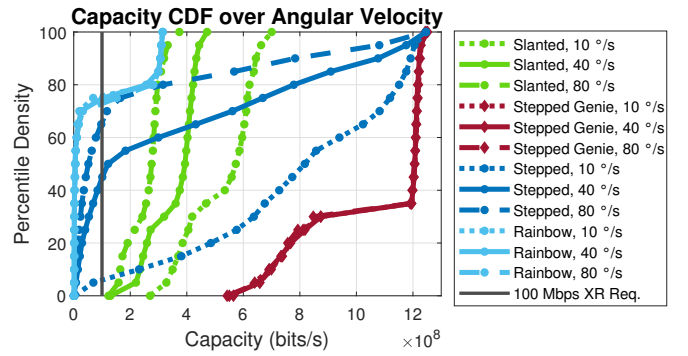


Fig. 9. Capacity CDFs for three UE velocities.

beam frequency selectivity and wider angular coverage. Our simulation results show that slanted beams provide more reliable coverage for multiple users over a specified angular range or for random movement. Slanted beams provided up to two orders-of-magnitude better minimum capacity compared to baseline beam designs. Future work based on this beamforming method includes multi-frame tracking and protocol augmentations to improve continuous tracking.

## REFERENCES

- [1] A. Marinšek *et al.*, "mmwave for extended reality: Open user mobility dataset, characterization, and impact on link quality," *IEEE Commun. Mag.*, vol. 62, no. 8, pp. 24–30, 2024.
- [2] S. Jayaprakasam *et al.*, "Robust beam-tracking for mmwave mobile communications," *IEEE Commun. Lett.*, vol. 21, no. 12, pp. 2654–2657, 2017.
- [3] B. W. Domae *et al.*, "Machine learning prediction for phase-less millimeter-wave beam tracking," in *2022 IEEE 23rd Int. Workshop on Signal Process. Advances in Wireless Commun. (SPAWC)*, 2022, pp. 1–5.
- [4] V. Va, H. Vikalo, and R. W. Heath, "Beam tracking for mobile millimeter wave communication systems," in *2016 IEEE Global Conf. on Signal and Information Process. (GlobalSIP)*, 2016, pp. 743–747.
- [5] H. Chung *et al.*, "Adaptive beamwidth control for mmwave beam tracking," *IEEE Commun. Lett.*, vol. 25, no. 1, pp. 137–141, 2021.
- [6] S. Zhou, L. Chen, and W. Wang, "Attitude information aided mmwave beam tracking based on codebook," *IEEE Commun. Lett.*, vol. 26, no. 5, pp. 1160–1164, 2022.
- [7] V. Boljanovic *et al.*, "Fast beam training with true-time-delay arrays in wideband millimeter-wave systems," *IEEE Trans. Circuits Syst. I*, vol. 68, no. 4, pp. 1727–1739, 2021.
- [8] H. Yan, V. Boljanovic, and D. Cabric, "Wideband millimeter-wave beam training with true-time-delay array architecture," in *2019 53rd Asilomar Conf. on Signals, Systems, and Comput.*, 2019, pp. 1447–1452.
- [9] V. V. Ratnam *et al.*, "Joint phase-time arrays: A paradigm for frequency-dependent analog beamforming in 6g," *IEEE Access*, vol. 10, pp. 73 364–73 377, 2022.
- [10] D. Zhao *et al.*, "Fast frequency-direction mapping design for data communication with true-time-delay array architecture," in *2024 Int. Conf. on Comput., Networking and Commun. (ICNC)*, 2024, pp. 1071–1076.
- [11] J. Mo *et al.*, "Mobility robustness using joint phase-time arrays," US Patent US20230362671A1, Nov., 2023.
- [12] G. Zhou *et al.*, "Radar rainbow beams for wideband mmwave communication: Beam training and tracking," *IEEE J. Sel. Areas Commun.*, vol. 43, no. 4, pp. 1009–1026, 2025.
- [13] M. Giordani *et al.*, "A tutorial on beam management for 3gpp nr at mmwave frequencies," *IEEE Commun. Surveys Tuts.*, vol. 21, no. 1, pp. 173–196, 2019.
- [14] K. H. Sayidmarie and Q. H. Sultan, "Synthesis of wide beam array patterns using quadratic-phase excitations," *Int. J. of Electromagnetics and Applicat.*, vol. 3, no. 5, pp. 127–135, 2013.
- [15] F. Alriksson *et al.*, "Future network requirements for extended reality applications," *Ericsson Technology Review*, Apr 2023.